Coarse woody debris features of a warm temperate deciduous broad-leaved forest, northern China

Fang Ma[1] · Liwen Zhuang[2] · Shunzhong Wang[3] ·
Weiguo Sang[1,3]

Abstract Stocking and structural composition of a deciduous broad-leaved forest were determined to predict coarse woody debris quantity by quantifying the empirical relationships between these two attributes. The most ecologically significant families by stem density were Salicaceae, Betulaceae, Fagaceae, and Aceraceae. *Populus davidiana* was the most dominant species followed by *Betula dahurica*, *Quercus mongolica*, and *Acer mono*. The four species accounted for 69.5% of total stems. Numerous small-diameter species characterized the coarse woody debris showing a reversed J-shaped distribution. The coarse debris of *P. davidiana*, *B. dahurica*, and *Q. mongolica* mainly comprised the 10–20 cm size class, whereas *A. mono* debris was mainly in the 5–10 cm size class. The spatial patterns of different size classes of coarse woody debris were analyzed using the g-function to determine the size of the tree at its death. The results indicate that the spatial patterns at the 0–50 m scale shifted gradually from an aggregated to a random pattern. For some species, the larger coarse debris might change from an aggregated to a random distribution more easily. Given the importance of coarse woody debris in forest ecosystems, its composition and patterns can improve understanding of community structure and dynamics. The aggregation pattern might be due to density dependence and self-thinning effects, as well as by succession and mortality. The four dominant species across the different size classes showed distinct aggregated distribution features at different spatial scales. This suggests a correlation between the dominant species population, size class, and aggregated distribution of coarse woody debris.

Keywords Tree mortality · Diversity · Size class · Forest dynamic plot

✉ Liwen Zhuang
  zlw9593@163.com

✉ Weiguo Sang
  swg@muc.ac.cn

1   Minzu University of China, No. 27, Zhongguancun Nandajie, Haidian District, Beijing 100081, People's Republic of China

2   Heilongjiang Academy of Forestry Science, No 134 Haping Road, Nangang District, Harbin 150081, People's Republic of China

3   Key Lab of Environment and Vegetation Change, Institute of Botany, Chinese Academy of Sciences, No. 20 Xiangshan Nanxincun, Haidian District, Beijing 100093, People's Republic of China

Introduction

Tree mortality is an important ecological process (Bin et al. 2011) and results in coarse woody debris (CWD) in various stages of decomposition, including fresh and rotting logs, snags, stumps, and large branches. Information on CWD can illustrate structural and functional components of forest ecosystems (Harmon et al. 1986; Spies et al. 1988). CWD has crucial roles in providing habitats for plants, animals, and fungi, in nutrient cycling and long-term carbon storage, species regeneration, and the maintenance of environmental heterogeneity and biological diversity (Harmon et al. 1986; Franklin 1991; Bunnell and Houde 2010; Stokland et al. 2012; Dittrich et al. 2014; Köster et al. 2015).

Species composition is the basis of community structure and helps to understand the long-term effects, development, and evolution of plant status in an area. Community structure reflects the heterogeneity of plant distribution in horizontal and vertical directions, and the spatial distribution of species reveals past ecological processes of the species and the maintenance mechanisms of species diversity. Similarly, knowing the composition, structure, and distribution patterns of coarse woody debris could provide information on the size of trees at mortality, their age, configuration, and species differences to better understand community dynamics and species maintenance mechanisms.

Since the establishment of the first large-scale forest dynamic plot (FDP) on Barro Colorado Island in Panama in 1980 (Ma 2008), there have been 20 fixed monitoring plots established in 15 countries and regions. The species compositions are high in FDPs, resulting in a large data set that can help understand the changes and impacts of biodiversity and the coexistence mechanisms of species. Community species composition, structure, and distribution in FDPs reveal information about zonal vegetation succession that can guide development of plans for biodiversity conservation. Over the past decade, several studies have related CWD characteristics with forest succession, community composition, nutrient cycling, and forest management (Idol et al. 2001; Montes and Cañellas 2006; Woodall and Nagel 2006; Sefidi et al. 2008). In addition, current knowledge regarding CWD and the associated underlying mechanisms in communities is mainly from tropical and subtropical forests. There is a lack of research on the distribution and abundance of CWD in temperate forests, particularly in northern China. The economic development of these forests has resulted in significant ecological damage. Only remnant old-growth forests remain, and most forest cover is secondary growth on previously forested land that has recovered from anthropogenic disturbances. Therefore, understanding the relation between CWD and its formative factors is important to understanding succession history and improving the conservation of secondary forests.

In this study, our objectives were to: (1) understand the characteristics of CWD species composition and diversity; (2) examine CWD structure; (3) determine the spatial distribution of CWD; and (4) analyze factors affecting CWD accumulation in warm temperate, deciduous broad-leaved secondary forests. We also discuss the implications of our results for predicting CWD and outline the need for future studies.

Methods and study site

The Dongling Mountains, hereinafter referred to as the Dongling Mountain plot or DLM (Fig. 1) are located in
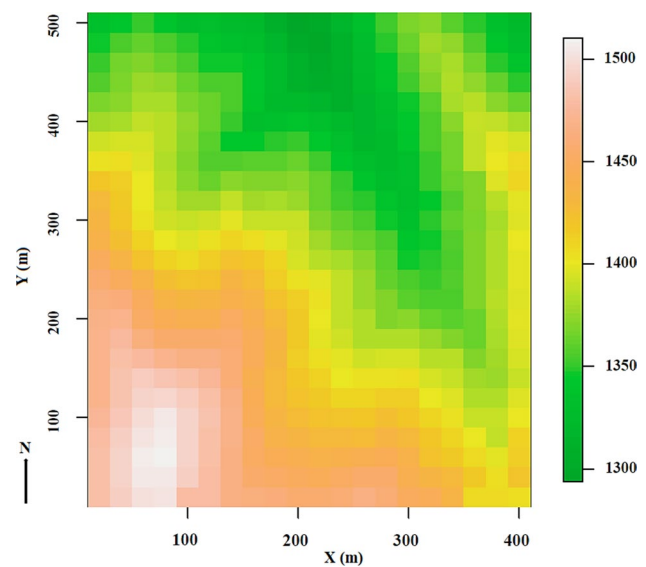

Fig. 1 Elevation at the 20-ha plot in Dongling Mountains

the center of the Beijing Xiaolongmen Forest Park Reserve (115° 26′ E, 40° 00′ N) The vegetation exhibits the features of warm temperate, deciduous broad-leaved forests, and the community structure is relatively complex. It is one of the first sites selected for study in China's warm temperate regions and has a warm temperate continental monsoon climate with four distinct seasons, with a mean annual temperature of 4.8 °C, an average July (hottest) temperature of 18.3 °C and an average January (coldest) temperature of − 10.1 °C. The annual frost-free period is approximately 195 days and annual sunshine is 2,600 h. Within the study area, annual precipitation is 500–650 mm, and occurs mainly during June, July and August, accounting for approximately 78% of annual precipitation. The parent soil material is mountain brown soil. The vegetation is typical warm temperate, deciduous broad-leaved secondary forest with excellent community structure (Dai et al. 2018). The tree species of the DLM plot consist of *Quercus mongolica*, *Betula dahurica*, *Acer mono, Populus davidiana*, and *Betula platyphylla*, accompanied by *Fraxinus rhynchophylla*, *Juglans mandshurica*, *Sorbus discolor*, *Tilia mongolica*, and *Ulmus macrocarpa*. Shrub communities mainly include *Syringa pubescens*, *Abelia biflora*, *Corylus mandshurica*, *Deutzia parviflora*, and *Rhododendron micranthum*.

Data collection

The 20-ha plot was divided into 10 m × 10 m subplots using the coordinates of the northwest corner as the origin, resulting in 500 subplots. For each subplot, species, height, diameter at breast height (DBH ≥ 1 cm), and coordinates of all

live woody species were recorded. Data collection was completed in 2010 (Liu et al. 2011).

In 2016, based on the 2010 data set, we further recorded DBH, length and coordinates of any dead trees with DBH ≥ 5 cm, and the decay class.

Statistical methodology

To determine species richness, the lists of woody species for each subplot were pooled. A species-area curve of the 20-ha plot, began with the original base point as the unit; the sampling area was gradually enlarged to encompass more tree species, calculated as a nest square shape based on combining and expanding samples, resulting in a species-area curve. A rank abundance curve was plotted as the abundance of each species against the rank of each species (Zhang et al. 2012).

To analyze the spatial point patterns of CWD, the univariate version of the pair correlation function $g(r)$ (Eq. 2) was used to interpret the coordinate data (Diggle 1983; Wiegand and Moloney 2010). The function $g(r)$ is derived from Ripley's K function (Eq. 1) (Loosmore and Ford 2006).

$$K(r) = \frac{A}{n^2} \sum_{i=1}^{n} \sum_{j=1}^{n} \frac{I_r(U_{ij})}{W_{ij}} (i \neq j) \tag{1}$$

$$g(r) = \frac{1}{2\pi r} \frac{dK(r)}{d(r)} \tag{2}$$

where, A is the plot area, n the total number of individuals in the plot, and U_{ij} the distance between two points i and j. When the distance u between the individuals i and j is $u \leq r$, $Ir(u)$ is 1, otherwise it is 0; W_{ij} is the proportion of the area of the circle with center is i and radius is d_{ij} in the area A.

The g function was computed using the Spatstat package in R (Baddeley and Rubak 2015). The distances used to calculate the g function ranged from 0 to 50 m. The maximum value of r was 50 m or half of each 100 m × 100 m plot, following Salas et al. (2006), Zhang et al. (2009a), and Kazempour et al. (2018). In addition, the 99 Monte Carlo simulation method was used to develop a 99% confidence interval envelope (Zhang et al. (2009b), Lu et al. 2015). The result corresponded to complete spatial randomness if $g(r) = 1$, aggregation at a distance of r if $g(r) > 1$, and regular distribution if $g(r) < 1$ (Bivand et al. 2013).

Results

CWD compositional diversity

CWD richness

We counted 7,137 stems (357 stems ha^{-1}) in the CWD ≥ 5 cm size class within the 20-ha plot, identified them to species level (7,075 individuals, 99.1%). These represented 33 species of 25 genera and 15 families. There were 32 morphospecies (ones based entirely on morphological features). With the exception of one gymnosperm (*Larix principis-rupprechtii* Mayr), all the other woody species were dicotyledons.

Table 1 lists the number of species in the four richest families. The most dominant families ranked in descending order as Salicaceae, Betulaceae, Fagaceae, and Aceraceae, with the relative density of the most dominant family being 31.7%, and the least dominant being 13.4%. At the species level, the most abundant species in descending order were *P. davidiana*, *B. dahurica*, *Q. mongolica*, and *A. mono*. These were distributed throughout the plot, collectively contributing 69.5% to the total number of species.

The species-abundance pattern showed that a few species contributed significantly and were dominant (> 1000 individuals) in the 20-ha plot (Fig. 2). The sum of ranks 1 through 4 was 4960 individuals, accounting for 69.5% of the total. From ranks 5 to 10, the curve had a shallow gradient, with the top 10 species accounting for 90% of the total. Among the 33 species, nine (1%) had < 20 individuals (< 1 ind. ha^{-1}), and two were represented by only a single individual.

The plot of the number of species was compared against the number of trees predicted by Eq. 3:

$$S = \alpha \ln (1 + N/\alpha) \tag{3}$$

Table 1 Top four families and species in the 20-ha plot in the Dongling Mountains

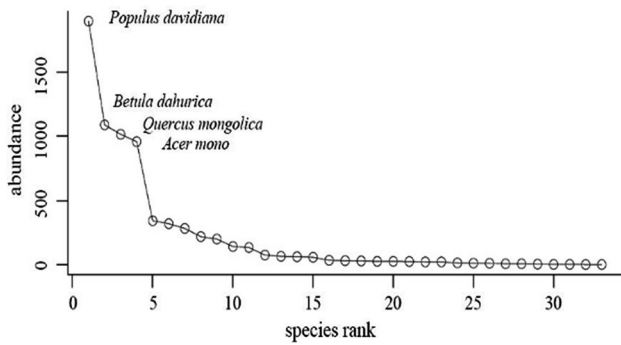| CWD families	Stems (ha^{-1})	Relative density (%)
Salicaceae	2194	31.7
Betulaceae	1443	20.2
Fagaceae	1015	14.2
Aceraceae	958	13.4
Other	1527	20.4
CWD dominant species	Stems	Relative density (%)
Populus davidiana	1898	26.6
Betula dahurica	1089	15.3
Quercus mongolica	1015	14.2
Acer mono	958	13.4
Other	2177	30.5

Fig. 2 Species-abundance curve for the Dongling Mountains Forest Dynamic Plot
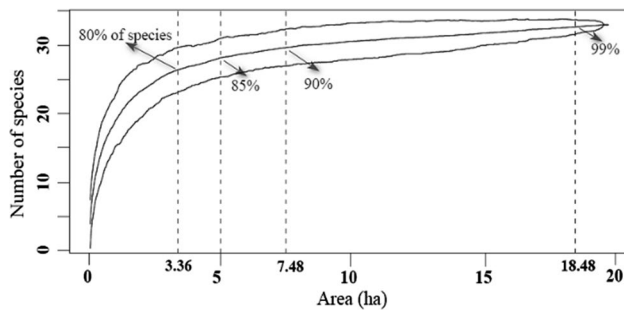
Fig. 3 Species-area curve for the 20-ha Donglings Mountains Forest Dynamics Plot

Fig. 4 Size class distribution for CWD in Dongling Mountains 20-ha plot
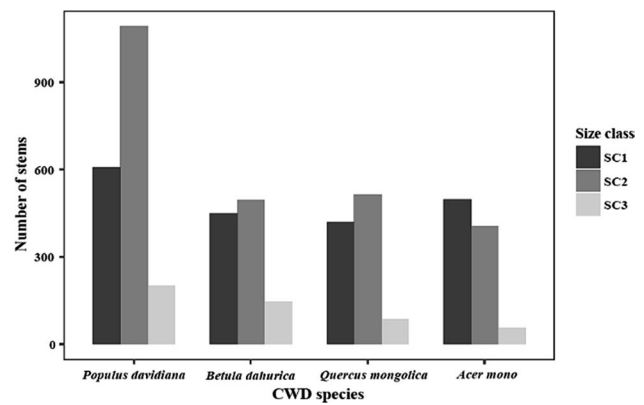
Fig. 5 Dominant species by CWD size class in the 20-ha plot in the Dongling Mountains

The number of species increased rapidly until the incline plot area reached 3.36 ha, when ~80% of the species had been accumulated (Fig. 3). The curve plateaued after sampling 5.0 ha and approached an asymptote. Few species (10%) were added after sampling 7.48 ha.

CWD structure

The CWD size class structure showed that sizes ‹ 40 cm had reversed J-shaped curves (Fig. 4). There was a decrease in abundance with increasing size class, although the inverse J-shaped curve indicated a steep decline in numbers with increasing size. The CWD distribution of the size classes showed that size class sc1 ($5 \leq$ sc1 < 10 cm) accounted for more than 42%, most individual coarse debris species were size class sc2 ($10 \leq$ sc1 < 20 cm), accounting for 49%, and those in size class sc3 (≥ 20 cm) accounted for 9% (Fig. 5).

Analysis of the diameter structure of the major dead species (Fig. 5) showed that *P. davidiana, B. dahurica* and *Q. mongolica* accounted for most of the intermediate class sc2 (≥ 10 cm), whereas *A. mono* was concentrated in the sc1 (5-cm size class). *P. davidiana* had the most individuals and thus, the impact of its dead wood on the community is larger than other species.
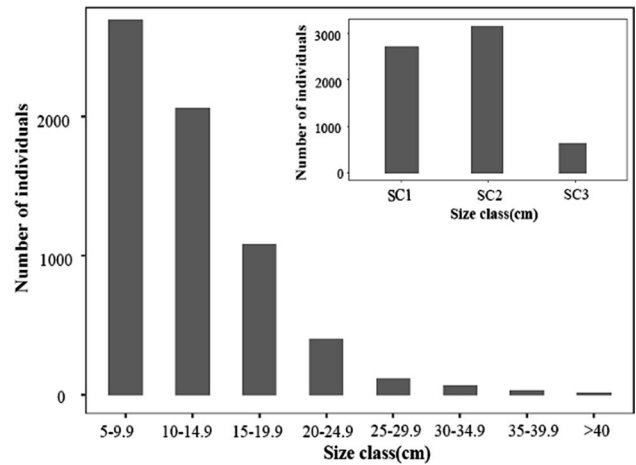
Spatial distribution

In the different size classes of a population, the distribution pattern varies over time. The *g*-function of a point pattern analyzes the variations in distribution patterns of tree species in different size classes. Our results showed that for three size classes, almost all species were clustered between 0 and 50 m, whereas with an increasing scale, the degree of clustering declined and became a random distribution ("Appendix" Fig. 6). No species had a regular distribution pattern under the CSR null model. In contrast, the degree of overall aggregation decreased gradually with increasing size class at the 0 to 50 m scale ("Appendix" Fig. 6), with the larger stems more randomly distributed.

P. davidiana and *A. mono* were mainly in the middle and southeast of the plot, *B. dahurica* in the corners, and *Q. mongolica*, common in secondary broad-leaf forests,

was throughout the plot except on the top of the mountain ("Appendix" Fig. 7). The spatial distribution of the same species in different size classes followed a clear pattern, with the exception of a shift in distribution from aggregation to random with increasing size class. The CWD of small-diameter species was mostly clumped from 0 to 50 m. The intermediate size class was randomly distributed with the exception of *B. dahurica*. The four dominant species were all significantly randomly distributed. Thus, the larger coarse woody debris size classes transitioned from an aggregated to a random distribution more easily, compared with smaller size classes.

Discussion

Given the numerous functions of coarse woody debris in terrestrial systems (Harmon et al. 1986), understanding its dynamics, distribution, and species identity in forest management is important. If woody debris is to be managed for the maintenance of biodiversity and/or to maintain certain stand structural characteristics or attributes, factors influencing CWD distribution and dynamics need to be identified. However, such an understanding is difficult because of the multitude of factors simultaneously influencing the input and decay of CWD.

Forest composition is the foundation of research into many forestry and forest ecology-related issues, and is a basic characteristic of forest ecological systems. CWD is an important element in forest functioning and productivity (Janisch and Harmon 2002; Laiho and Prescott 2004), although little is known about the compositional diversity of CWD.

The abundance of coarse woody debris is a reflection of the composition and structural characteristics of stands, and tree species composition affects CWD diversity because it influences stand productivity and structure (Brassard and Chen 2008). Highly productive stands have more diverse tree species and consequently, more diverse CWD composition compared with stands with low productivity. For example, the low levels of deciduous coarse debris in boreal forests is explained by the low number of deciduous species (Kneeshaw et al. 2011).

CWD richness

The mean density of CWD in our forest dynamic plot forest was 357 ind. ha^{-1}, compared to an average of 405 ind. ha^{-1} in a *Nothofagus-Araucaria* mixed forest in Rucachoroy, Argentina (Szymañski et al. 2016). In a temperate deciduous forest in Iran, the amount of deadwood was 462 ind. ha^{-1} (Mataji et al. 2014). In the current study, we found low amounts of CWD, which differs from what was expected in the FDP.

In other plots, fire, windthrow and dieback resulting from insect outbreaks can result in high levels of CWD. In the Dongling Mountains plot, the low volumes of coarse woody debris can be explained by the general attributes of secondary forests; trees are relatively young and there is a lack of large dead ones. In addition, quantities of CWD depend on other factors such as geographical location and forest management (Stevenson et al. 2006; Woodall and Liknes 2008). Our study area was subject to considerable human interference as dead wood was collected for fuel and as raw material for manufacturing.

In the Dongling Mountains FDP, there was no correlation between the number of standing trees and CWD at the family level. Species of the Rosaceae, Salicaceae, and Betulaceae were common both as living and dead trees. There was no similarity between the deadwood of Caprifoliaceae and Saxifragaceae in terms of their impact on tree diversity; this might be related to their unique life histories and the ecological niches they occupy (Iida et al. 2011). Individuals of *Abelia biflora*, *Syringa pubescens* and *Corylus mandshurica* were significantly more abundant than were those of other species, but this was not the case for species richness as reflected in the CWD. Many species of these two families are small shrubs, characterized by fast growth and great abundance, and are in the shrub layer, requiring low resource levels to support their growth. The densities of species including *Populus davidiana, Betula dahurica, Fraxinus rhynchophylla,* and *Quercus mongolica* were reflected in the coarse woody debris because they are pioneer and dominant species and because of their reproductive strategies and status in succession. Pioneer species, such as *P. davidiana*, have initially high survival and rapid growth rates, but with succession, pioneer species gradually become fewer in number and form most of the CWD. The warm temperate deciduous broad-leaved forest in the Dongling Mountains plot is secondary vegetation that has successfully established in an area that was previously forested. When interpreting species-area curves, it should be noted that the study area was a 20-ha plot. Large study areas include more spatial and environmental heterogeneity, which can result in biases when comparing results with those from smaller study areas (Collins and Simberloff 2009), and can lead to over- or under-estimates of CWD diversity. In the current study, the number of species sharply increased initially with increasing area, and then slowly and gradually increased, resulting in relatively smooth species-area curves, especially for the total area. This is an indication that the sample sizes were sufficient and the plot area adequately represented the species composition of the vegetation.

CWD structure

The spatial patterns of deadwood in each species diameter class were different and they reflect the relationship between growth and the environment. The diameter structure of deadwood can explain the driving forces of forest development, predict directions of succession, and reveal age variations of the population. In the current study, stems in the < 20 cm size class accounted for 91% of CWD, which is similar to that reported for a mountain beech forest in New Zealand (Coomes and Allen 2010). Our result is also consistent with the distribution of deadwood size structure in Changbai Mountain broad-leaved Korean pine forests, Badagongshan evergreen broad-leaved forests, and Nonggang Kasht seasonal rain forests (Wang et al. 2011, 2014; Lu et al. 2015).

Species composition of CWD varied by size class. Mortality rate decreased with increasing diameter because large trees were more resistant to environmental pressures compared with smaller trees.

Spatial distribution

There was a close relationship between the spatial patterns of species and ecological processes. The study of population patterns can not only describe the population structure but also explain the causes of the pattern and clarify the dynamics of populations and communities. Given that patterns in the size classes of CWD vary (Iida et al. 2011), the study of the class structure of fallen trees can reveal cases of 'success-driven death' (Bond Lamberty et al. 2014). In the current study, the spatial pattern of coarse woody debris was on a scale of 0–50 m. The analysis of the distribution of three size classes ($\geq 5; \geq 10; \geq 20$) of all species revealed an aggregated distribution that became more random as the scale increased. These results are consistent with research on the distribution patterns of dead trees in the Badagong Mountains of Hunan Province, China, which showed that small woody debris tended to be aggregated, whereas larger CWD was more randomly distributed (Lu et al. 2015). Our results are also similar to those reported for aging European *Picea abies* (L.) H. Karst forests (Fraver et al. 2008) and in Arizona, USA. The aggregation pattern of CWD might be the results of density and self-thinning but might also result from succession and natural death.

There was no obvious pattern to the spatial distributions of CWD species in different size classes because of the impact of growth, survival and competition between species in different microenvironment conditions (Frelich et al. 1993; Gong et al. 2013). Thus, the type of species was not the key factor restricting the spatial distribution patterns of tree species in our study plot. However, the four most dominant species across the size classes showed distinct aggregated distribution features at different scales. This suggests a correlation between the dominant species population, size class, and aggregated distribution of coarse woody debris.
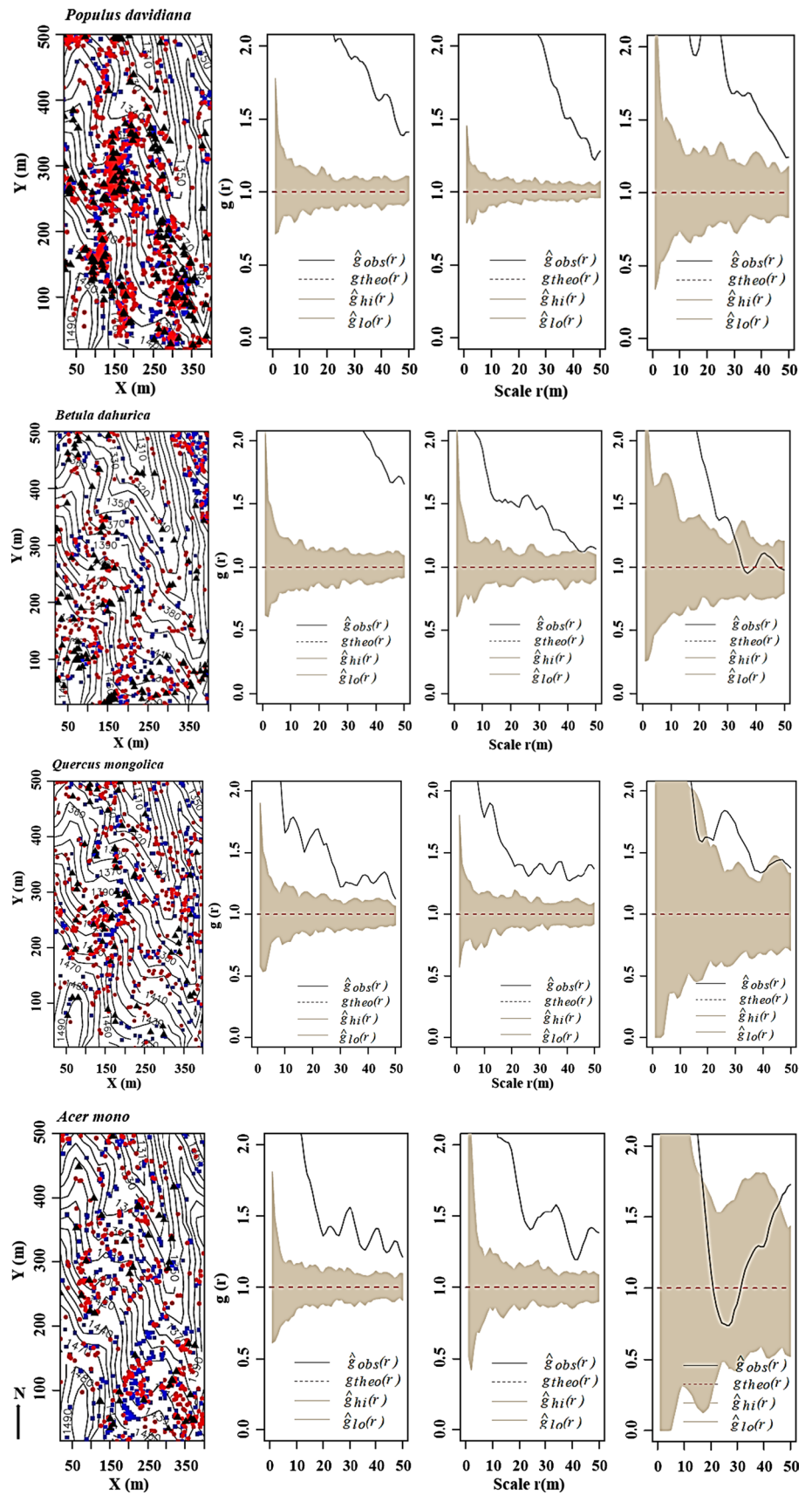
Appendix 1

See Fig. 6.

Fig. 6 Spatial distribution patterns of dead wood species in different size class. **a**: $5 \leq SC < 10$; **b**: $10 \leq SC < 20$ cm; **c**: $SC \geq 20$ cm
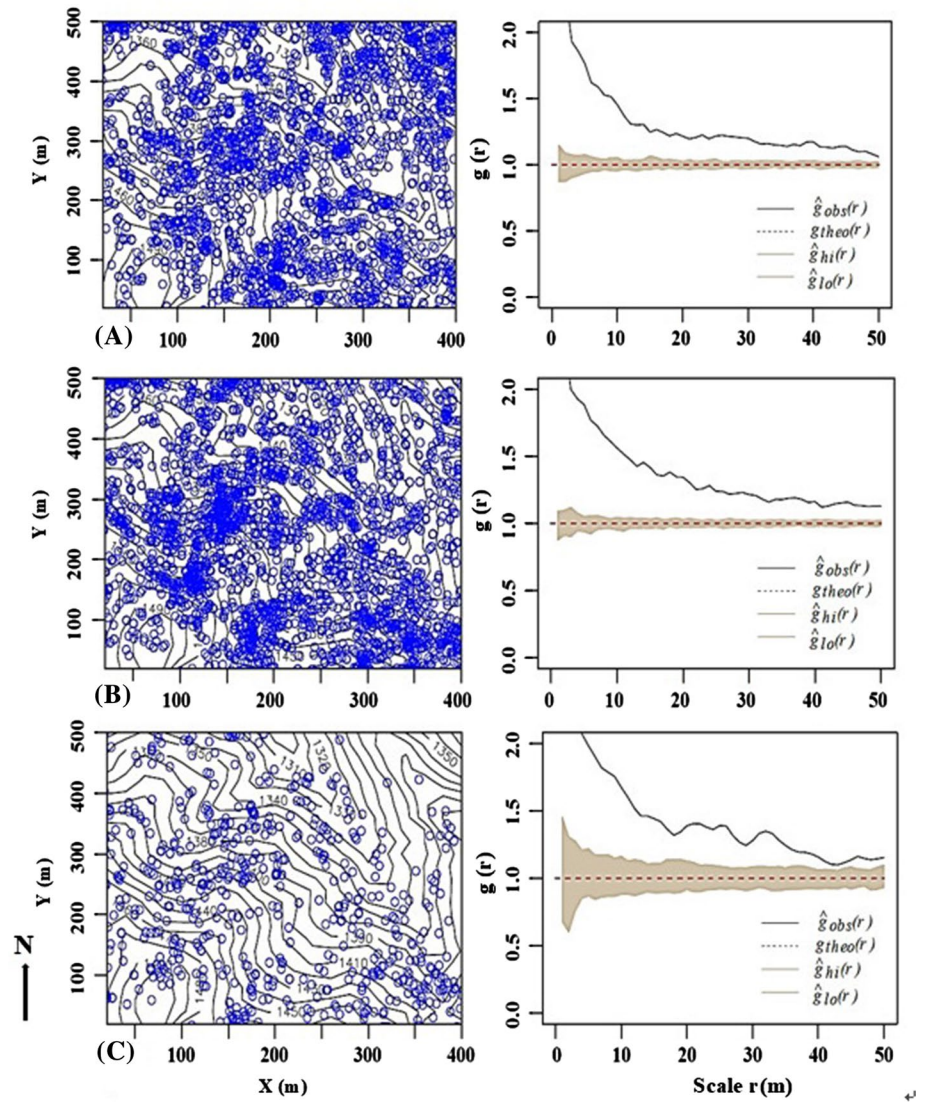
Appendix 2

See Fig. 7.

Fig. 7 Spatial distribution maps of four dominant canopy species in the 20-ha plot of the Dongling Mountains. Square: SC ≥ 20 cm; Circle: 10 ≤ SC < 20 cm; Traingle: 5 ≤ SC < 10

References

Baddeley A, Rubak E, Turner R. 2015. Spatial point patterns: methodology and applications with R. London: Chapman and Hall/CRC Press. https://www.crcpress.com/Spatial-Point-Patterns-Methodology-and-Applications-with-R/Baddeley-Rubak-Turner/9781482210200/. Accessed 15 Sept 2018

Bin Y, Lian J, Wang Z, Ye W, Cao H (2011) Tree mortality and recruitment in a subtropical broadleaved monsoon forest in south china. J Trop For Sci 23:57–66

Bivand RS, Pebesma E, Gómez-Rubio V (2013) Spatial point pattern analysis. applied spatial data analysis with R. Springer, New York, pp 173–211

Bond Lamberty B, Rocha AV, Calvin K, Holmes B, Wang C, Goulden ML (2014) Disturbance legacies and climate jointly drive tree growth and mortality in an intensively studied boreal forest. Glob Change Biol 20:216–227

Brassard BW, Chen HY (2008) Effects of forest type and disturbance on diversity of coarse woody debris in boreal forest. Ecosystems 11:1078–1090

Bunnell FL, Houde I (2010) Down wood and biodiversity-implications to forest practices. Environ Rev 18:397–421

Collins MD, Simberloff D (2009) Rarefaction and nonrandom spatial dispersion patterns. Environ Ecol Stat 16:89–103

Coomes D, Allen R (2010) Mortality and tree-size distributions in natural mixed-age forests. J Ecol 95:27–40

Dai W, Fu W, Jiang P, Zhao K, Li Y, Tao J (2018) Spatial pattern of carbon stocks in forest ecosystems of a typical subtropical region of southeastern China. For Ecol Manage 409:288–297

Diggle PJ (1983) Statistical analysis of spatial point patterns. Biometrics 32:659–667

Dittrich S, Jacob M, Bade C, Leuschner C, Hauck M (2014) The significance of deadwood for total bryophyte, lichen, and vascular plant diversity in an old-growth spruce forest. Plant Ecol 215:1123–1137

Franklin JF (1991) Composition, function, and structure of old-growth Douglas-fir forests. Wildlife and vegetation of unmanaged Douglas-fir forests. USDA Forest Service, Washington, D.C., pp 71–80

Fraver S, Jonsson BG, Jönsson M, Esseen PA (2008) Demographics and disturbance history of a boreal old-growth Picea abies forest. J Veg Sci 19:789–798

Frelich LE, Calcote RR, Davis MB, Pastor J (1993) Patch formation and maintenance in an old-growth hemlock-hardwood forest. Ecology 74:513–527

Gong H, Ye W, Hu X, Yang X (2013) Tree species diversity and related mechanism in an evergreen broad-leaved forest in Ailao Mountains, Yunnan, China. J Agric Res 8:134–144

Harmon ME, Franklin JF, Swanson FJ, Sollins P, Gregory SV, Lattin JD, Anderson NH, Cline SP, Aumen NG, Sedell JR (1986) Ecology of coarse woody debris in temperate ecosystems. Adv Ecol Res 15:133–302

Idol TW, Figler RA, Pope PE, Ponder Jr F (2001) Characterization of coarse woody debris across a 100-year chronosequence of upland oak-hickory forests. For Ecol Manage 149:153–161

Iida Y, Kohyama TS, Kubo T, Kassim AR, Poorter L, Sterck F, Potts MD (2011) Tree architecture and life-history strategies across 200 co-occurring tropical tree species. Funct Ecol 25:1260–1268

Janisch JE, Harmon ME (2002) Successional changes in live and dead wood carbon stores: implications for net ecosystem productivity. Tree Physiol 22:77–89

Kazempour LM, Taheri AK, Hassan P, David P, Beitollah A (2018) Spatial patterns of trees from different development stages in mixed temperate forest in the Hyrcanian region of Iran. J For Sci 64:260–270

Kneeshaw D, Bergeron Y, Kuuluvainen T (2011) Forest ecosystem structure and disturbance dynamics across the circumboreal forest The sage handbook of biogeography. Sage, Los Angeles, pp 263–280

Köster K, Metslaid M, Engelhart J, Köster E (2015) Dead wood basic density and the concentration of carbon and nitrogen for main tree species in managed hemiboreal forests. For Ecol Manage 354:35–42

Laiho R, Prescott CE (2004) Decay and nutrient dynamics of coarse woody debris in northern conifer. Can J for Res 34:763–777

Liu HF, Li L, Sang WG (2011) Species composition and community structure of the Donglingshan forest dynamic plot in a warm temperate deciduous broad-leaved secondary forest, China. Biodivers Sci 19:232–242

Loosmore NB, Ford ED (2006) Statistical inference using the g or K point pattern spatial statistics. Ecology 87:1925–1931

Lu ZJ, Liu FL, Wu H, Jiang MX (2015) Species composition, size class, and spatial patterns of snags in the Badagongshan (BDGS) mixed evergreen and deciduous broad-leaved forest in central China. Biodivers Sci 23:167–173

Ma KP (2008) Large scale permanent plots: important platform for long term research on biodiversity in forest ecosystem. J Plant Ecol 32:237–237

Mataji A, Sagheb-Talebi K, Eshaghi-Rad J (2014) Deadwood assessment in different developmental stages of beech (Fagus orientalis Lipsky) stands in Caspian forest ecosystems. Int J Environ Sci Technol 11:1215–1222

Montes F, Cañellas I (2006) Modelling coarse woody debris dynamics in even-aged Scots pine forests. For Ecol Manage 221:220–232

Salas C, Lemay V, Núñez P, Pacheco P, Espinosa A (2006) Spatial patterns in an old-growth Nothofagus obliqua forest in south-central Chile. For Ecol Manage 231:38–46

Sefidi K, Marvi MM, Zobeyri M, Etemad V (2008) Investigation on dead trees effects on natural regeneration of oriental beech and hornbeam in a mixed beech forest. Iran J F Poplar Res 4:365–373

Spies TA, Franklin JF, Thomas TB (1988) Coarse woody Debris in Douglas-Fir forests of western oregon and Washington. Ecology 69:1689–1702

Stevenson SK, Jull MJ, Rogers BJ (2006) Abundance and attributes of wildlife trees and coarse woody debris at three silvicultural systems study areas in the Interior Cedar-Hemlock Zone, British Columbia. For Ecol Manage 233:176–191

Stokland JN, Siitonen J, Jonsson BG (2012) Biodiversity in dead wood. For Chron 88:660–660

Szymañski C, Fontana G, Sanguinetti J (2016) Natural and anthropogenic influences on coarse woody debris stocks in Nothofagus—Araucaria forests of northern Patagonia. Argent Aust Ecol 42:48–60

Wang LW, Li BH, Ye J, Bai XJ, Yuan ZQ, Xing DL, Ling F, Shi S, Wang XG, Hao ZQ (2011) Dynamics of short-term tree mortality in broad-leaved Korean pine (Pinus koraiensis) mixed forest in the Changbai Mountains. Biodivers Sci 19:260–270

Wang B, Xiang WS, Ding T, Huang FZ, Wen SJ, Li DX, Guo YL, Li XK (2014) Spatial distribution of standing dead trees abundance and its impact factors in the karst seasonal rain forest, Nonggang, southern China. Chin Sci Bull 59:3479–3490

Wiegand T, Moloney KA (2010) Rings, circles, and null-models for point pattern analysis in ecology [Review]. Oikos 104:209–229

Woodall CW, Liknes GC (2008) Climatic regions as an indicator of forest coarse and fine woody debris carbon stocks in the United States. Carbon Balance Manage 3:5

Woodall CW, Nagel LM (2006) Coarse woody type: a new method for analyzing coarse woody debris and forest change. For Ecol Manage 227:115–121

Zhang J, Hao Z, Sun IF, Song B, Ye J, Li B, Wang X (2009a) Density dependence on tree survival in an old-growth temperate forest in northeastern China. Ann For 66:204

Zhang QY, Zhang YC, Peng SL, Yirdaw E, Ning W (2009b) Spatial structure of alpine trees in Mountain Baima Xueshan on the southeast Tibetan Plateau. Silva fennica 43:197–208

Zhang ZH, Hu G, Zhu JD, Ni J (2012) Stand structure, woody species richness and composition of subtropical karst forests in Maolan, south-west China. J Trop For Sci 24:498–506

Publisher's Note Springer Nature remains neutral with regard to jurisdictional claims in published maps and institutional affiliations.